Chapter 3

RNA-Seq profiling of leukocyte populations and mycobacterium-infected cells from wild type and *ptpn6*-deficient zebrafish larvae

Zakia Kanwal, Julien J. Y. Rougeot, Anna Zakrzewska, Hans J. Jansen, Herman P. Spaink, and Annemarie H. Meijer

Abstract

The zebrafish is an excellent model for studying inflammatory and infectious diseases due to the optical transparency of its embryonic and larval stages and the availability of transgenic reporter lines that express fluorescent proteins in different leukocyte subtypes. However, the gene expression signatures of myeloid and lymphoid cell types in zebrafish and homologies with the human system are still largely unknown. Here we performed RNA-Seq profiling of eGFP-positive macrophages, neutrophils, and early T-cells from zebrafish larvae, which were obtained by fluorescence activated cell sorting (FACS) of transgenic *mpeg1:egfp*, *mpx:egfp*, and *lck:egfp* lines. Our RNA-Seq analysis resulted in comprehensive gene signatures for the different cell types and gave insight in genes that are more abundant or more specific than the currently used markers and thus highly useful for developing new reporter lines and lineage-specific antibodies. *Mycobacterium marinum*, which infects and persists in macrophages, markedly altered the gene expression signature of this cell type. *M. marinum*-infected cells displayed a general down-regulation of macrophage marker genes, along with up-regulation of ribosomal protein genes and genes involved in oxidative phosphorylation, proteolysis, ion transport, chromatin assembly, lipid metabolism, carbohydrate binding, and immunosuppression. The macrophage gene signature was also specifically altered under knockdown conditions of *ptpn6*, a protein tyrosine phosphatase gene known as a negative regulator of immune responses. In particular, deficiency of *ptpn6* resulted in a strong up-regulation of matrix metalloproteinase genes *mmp9* and *mmp13a* in uninfected macrophages as well as in *M. marinum*-infected cells. The up-regulation of these genes may be a major cause of the inflammatory phenotype and increased *M. marinum* susceptibility of *ptpn6*-deficient zebrafish larvae.

Introduction

The processes that occur during inflammation and immune responses to combat infection are orchestrated by complex changes in the gene expression profiles of different immune cell populations (Chaussabel et al., 2010). The analysis of cellular transcriptomes has been greatly advanced by recent developments in deep sequencing technology (Wang et al., 2009; Martin and Wang, 2011). RNA sequencing (RNA-Seq) is a powerful method to characterize transcriptional landscapes and discover novel transcripts or alternative splice forms (Cloonan et al., 2008; Mortazavi et al., 2008; Nagalaskhmi et al 2008; Sultan et al., 2008; Trapnell et al., 2010). RNA-Seq has also proved to be an accurate method for quantitative analysis of differential gene expression (Mortazavi et al., 2008). In this respect, RNA-Seq analysis has several advantages over microarray technology, including a higher sensitivity, a lower background, and independency of prior knowledge of the transcriptome (Marioni et al., 2008; Malone and Oliver, 2011). In RNA-Seq analysis, cDNA read lengths of over a hundred nucleotides can now routinely be obtained with the use of paired-end technology to link the ends of short cDNA fragments (Fullwood et al., 2009). These

reads are subsequently aligned to a reference database of exons or transcripts, and read count data is compared between samples using different statistically algorithms in R/Bioconductor packages such as DESeq, DEGseq, bayseq, and EdgeR (Anders and Huber, 2010; Hardcastle and Kelly, 2010; Robinson et al., 2010; Wang et al., 2010). The application of RNA-Seq technology has great potential to advance the understanding of the immune system during health and disease.

The immune system of vertebrates consists of two cooperative components, the innate and adaptive immune system (Janeway and Medzhitov, 2002). The innate immune response, which forms the first line of defence against infections, is initiated by phagocytic cells such as macrophages and neutrophils. In zebrafish embryos, these cells are the first to develop and consequently, the fish are solely dependent on their innate immune system during the early life stages (Herbomel et al., 1999; Le Guyader et al., 2008; Ellet and Lieschke, 2010). The first cells of the adaptive immune system, expressing early T-cell markers, can be detected by 4 days post fertilization (dpf), after the larval thymus is invaded by hematopoietic precursor cells (Kissa et al., 2008). However, the adaptive immune system is not considered to be functional until the fish reach several weeks of age (Lam et al., 2004). Therefore, zebrafish embryo and larval models are well suited for studies that specifically address the function of the innate immune defenses. Owing to the transparency of zebrafish at these early life stages, high-resolution imaging of the behavior of immune cells and interaction with pathogens is possible using fluorescent transgenic reporter lines (Hall et al., 2009). Furthermore, the combination of efficient forward and reverse genetics makes the zebrafish a very powerful model system (Lawson and Wolfe, 2011). Exploiting these unique advantages, many embryo/larval-based zebrafish models for human inflammatory and infectious diseases have recently been developed and are contributing to a better understanding of human disease mechanisms (Renshaw et al., 2007; Meeker and Trede, 2008; Meijer and Spaink, 2011; Oehlers et al., 2011; Renshaw and Trede, 2012).

In our previous work, transcriptome responses of zebrafish embryos during infection were analyzed at the whole organism level (Stockhammer et al., 2009; Stockhammer et al., 2010; van der Sar et al., 2009; Ordas et al., 2011; van Soest et al., 2011; Van der Vaart et al., 2012). In addition, we determined an expression profile of early myeloid precursor cells obtained from one-day-old embryos by fluorescence activated cell sorting (FACS) of a *spi1:egfp* transgenic line (Zakrzewska et al., 2010). Other recently developed fluorescent reporters can now be used for cell-specific analysis of different immune cell populations in zebrafish larvae. In this study, we used *mpeg1:egfp* (Ellett et al., 2011), *mpx:egfp* (Renshaw et al., 2006), and *lck:egfp* (Langenau et al., 2004) transgenic lines to determine the expression profiles of macrophages, neutrophils, and early T-cells, respectively. In addition, we used the mCherry marker present in a *Mycobacterium marinum* strain to isolate and profile infected cells from zebrafish larvae. Using an ultra-low input cDNA amplification method we could obtain libraries for Illumina RNA-Seq analysis from RNA quantities down to 100-200 pg. To detect transcripts that are induced under pathological inflammatory conditions, we also analyzed the profiles of macrophages, neutrophils, immature T-cells, and *M. marinum*-

infected cells under knockdown conditions of the *ptpn6* gene. This gene encodes a protein tyrosine phosphatase (Shp1) that is conserved between human and zebrafish and that functions as a negative regulator of the innate immune response (An et al., 2008; Croker et al., 2008; Chapter 2). The knockdown of *ptpn6* in zebrafish was previously shown to enhance the expression of pro-inflammatory genes and to result in a hyperactivation of the innate immune response during infection (Chapter 2). Our current data show a major effect of *ptpn6* knockdown on matrix metalloproteinase gene expression in uninfected macrophages as well as *M. marinum*-infected cells.

Materials and Methods

Zebrafish husbandry

Zebrafish were handled in compliance with the local animal welfare regulations and maintained according to standard protocols (zfin.org). Zebrafish lines used in this study included AB/TL, *Tg(mpx:egfp)i114* (Renshaw et al., 2006), *Tg*(*mpeg1:egfp)gl22* (Ellett et al., 2011) and Tg(*lck:egfp)cz2* (Langenau et al., 2004). Embryos were grown at 28.5–30°C in egg water (60 µg/ml Instant Ocean sea salts). For the duration of bacterial injections embryos were kept under anesthesia in egg water containing 200 µg/ml tricaine (Sigma-Aldrich).

Morpholino knockdown

Morpholino oligonucleotides (Gene Tools) were diluted to the desired concentration in 1× Danieau buffer (58 mM NaCl, 0.7 mM KCl, 0.4 mM $MgSO_4$, 0.6 mM $Ca(NO_3)_2$, 5.0 mM HEPES; pH 7.6) containing 1% phenol red (Sigma-Aldrich) and approximately 1 nl was injected at the 1-2 cell stage using a Femtojet injector (Eppendorf). For knockdown of *ptpn6* a splice morpholino targeting the exon 11/intron 11-12 splice junction (*ptpn6* MO1: 5'ACTCATTCCTTACCCGATGCGGAGC3'; 0.0625 mM) was used (Chapter 2).

Infection experiments

For infection experiments, a Mma20 strain of *Mycobacterium marinum* expressing mCherry in a pSMT3 vector was used (van der Sar et al., 2004). Glycerol stocks of the bacteria were prepared as described by Benard et al., (2012) and microinjected into the caudal vein of embryos at 28 hours post fertilization (hpf), using a dose of 100-150 CFU per embryo. After injections, embryos were transferred to fresh egg water and incubated at 28°C.

Fluorescent Activated Cell Sorting (FACS)

Macrophages, neutrophils and early lymphocytes from 5-6 dpf larvae were isolated by FACS as described in Cui et al. (2011). Briefly, live embryos were rinsed in calcium free Ringer for 15 min. Digestion was performed with 0.25% trypsin for 60-90 min at 28°C. Digestion was stopped with 1 mM $CaCl_2$ and 10% fetal calf serum. The resultant single cell suspension was centrifuged and washed with PBS and resuspended in Leibovitz

medium L15 supplemented with 1% fetal calf serum, 0.8 mM CaCl2, 50 units/ml penicillin and 0.05 mg/ml streptomycin. FACS was performed at 4°C using FACSAriaIII (BD Biosciences) with the BD FACSDiva software (version 6.1.3). For collecting mCherry-positive cells a Coherent Sapphire solid-state 561 nm yellow green laser with 36 mW power was used. Laser settings applied were 600LP, 615/20 BP. For sorting EGFP positive cells a Coherent Sapphire solid-state 488 nm laser with 15.4 mW power was used. Laser settings applied were 505 LP, 530/30 BP. The percentage of mCherry-positive cells in the life gate of cell suspensions from Mma20-infected embryos (from ±200 embryos) was between 0.1 to 1% over a time of ±25 min. The percentages of eGFP-positive cells in the life gate were: 0.09-0.2% over a time of ±20 min for lck:egfp cell suspensions (from ±150 embryos), 0.02-0.04% over a time of ±30 min for mpx:egfp cell suspensions (from ±250 embryos), and 0.04-0.1% over a time of ±25 min for mpeg1:egfp cell suspensions (from ±250 embryos). For negative controls in all cases a maximum of 500,000 non-fluorescent cells were obtained from the whole cell suspension. Fluorescent and non-fluorescent cell fractions were separately collected in supplemented L15 medium with addition of 10% zebrafish embryo extract (ZFIN) and RNA isolation was performed directly after sample collection.

RNA isolation and Illumina sequencing

RNA extraction of the cell fractions was done using the RNAqueous-Micro Kit (Ambion). RNA quality was checked by lab-on-a-chip analysis with an Agilent Bioanalyzer 2100 using the RNA 6000 Pico kit (Agilent, Santa Clara). RNA samples from non-fluorescent cell fractions had RIN values above 8. RNA integrity of samples from fluorescent cells was judged by the presence of ribosomal peaks in lab-on-a-chip analysis, but the quantity was generally too low for an accurate estimation of the RIN value and concentration. A total of 50 pg to 10 ng of RNA was used to make RNA-Seq libraries, using the Clontech SMARTer Ultra Low RNA Kit for Illumina Sequencing according to the manufacturer's instructions (Clontech Laboratories, Inc. Mountain View, CA, USA). After shearing the cDNA the Illumina TruSeq DNA Sample Preparation Kit v2 (Illumina Inc., San Diego, USA) was used to make the libraries. In the manufacturer's instructions three modifications were made. In the adapter ligation step the adapters were diluted 20-fold. In the library size selection step the library fragments were isolated with a double Ampure XP purification with a 0.7x beads to library ratio. The library amplification step was done with 15 cycles. The resulting mRNA-Seq library was sequenced using an Illumina HiSeq2000 instrument according to the manufacturer's description with a read length of 2 x 50 nucleotides. Image analysis and base calling was done by the Illumina HCS version 1.15.1. Sequence reads were quality trimmed using the quality_trim module in the CLCbio Assembly Cell v4.0.6. Filtered reads were mapped to Ensembl transcripts (Zv9_63) using the ref_assemble_short module in the CLCbio Assembly Cell v4.0.6. Accumulation of transcripts to Ensembl genes was done by first converting the mapping files to a table with the assembly_table module in the CLCbio Assembly Cell v4.0.6. Secondly, a custom script was used that sums all reads

belonging to the same gene. Non-uniquely mapped reads were divided between genes according to their ratio of uniquely mapped reads. Finally, read counts of transcripts belonging to the same gene were summed to obtain count data at Ensembl gene level. Fold-change and differential expression significance values were calculated from gene level read counts using the DESeq package (version 1.8.3) available in Bioconductor (version 2.10). DESeq utilizes a negative binomial distribution for modeling read counts per gene and implements a method for normalizing the counts (Anders and Huber, 2010).

Results and Discussion

RNA-Seq analysis of FACS-sorted macrophages from *mpeg1:egfp* transgenic zebrafish

To determine a gene expression signature for macrophages, we took advantage of a recently described zebrafish line that expresses enhanced GFP (eGFP) under control of the *mpeg1* gene promoter (Ellett et al., 2011). For isolation of eGFP-labeled macrophages we dissociated 5 or 6 day old larvae by trypsinization and subjected the resulting single cell suspensions to FACS sorting. The eGFP-labeled cells constituted between 0.04 to 0.1% of the total cell population and by sorting for 25 min we could obtain 4000-10,000 eGFP-labeled cells from pools of approximately 250 dissociated larvae. After testing different RNA isolation methods, we concluded that the RNAqueous-Micro Kit (Ambion) yielded good quality RNA from such small quantities of cells. The SMARTer Ultra Low RNA Kit for Illumina Sequencing was used to make RNA-Seq libraries. We succeeded in making RNA-Seq libraries even from samples with an estimated RNA input below 100 pg, where ribosomal peaks were just above the detection limit of lab-on-a-chip analysis with the RNA 6000 Pico kit. Approximately 10 million paired-end reads were obtained per library. To determine the reproducibility of the method we compared the results of RNA-Seq analysis of 4 biological replicates. For each replicate DESeq analysis identified several hundreds of genes with enriched expression in the eGFP-positive cell fraction versus the eGFP-negative fraction. Pairwise comparison of the replicates showed an overlap of around 50% of significant genes between each pair, and 29% of the significant genes were common to all 4 replicates (Supplementary Table 1). This demonstrates that consistent results can be obtained from RNA-Seq analysis of FACS-sorted eGFP-labeled macrophages, despite that there are many steps in the procedure where variation can be introduced (different pools of embryos, dissociation and FACS sorting, cDNA amplification from ultra low RNA start material). By combining the 4 replicates, which increases the statistical power of DESeq analysis (Anders and Huber, 2010), we identified a total of 925 genes with significantly enriched expression in macrophages (Supplementary Table 2). As expected, gene ontology analysis using DAVID (Huang et al., 2009) showed specific enrichment of KEGG pathways and GO-terms related to the immune system (Table 1).

Table 1. KEGG pathways and Gene Ontology terms enriched in macrophage and neutrophil cell fractions*

Category	Term	Fold Enrichment	
		mpeg1+	mpx+
KEGG pathways	cytokine-cytokine receptor interaction	4,4	4,6
	lysosome	4,1	
	Toll-like receptor signaling pathway	4,6	
	natural killer cell mediated cytotoxicity	4,6	
	intestinal immune network for IgA production	8,9	
	NOD-like receptor signaling pathway	5,4	7,8
	Jak-STAT signaling pathway	3,2	
	apoptosis	3,3	
	VEGF signaling pathway	3,3	
GO:Biological Process	immune response	5,4	
	defense response	7,2	8,0
	innate immune response	9,8	
	response to bacterium	7,4	16,6
	ntigen processing and presentation	5,2	
	chemotaxis	16,8	
GO:Molecular Function	cytokine binding	8,6	
	cysteine-type endopeptidase activity	5,2	
	peptidase activity, acting on L-amino acid peptides	2,2	2,9
	nucleotide receptor activity, G-protein coupled	9,5	
	purinergic nucleotide receptor activity, G-protein coupled	9,5	
	peptidase activity	2,1	2,8
	cysteine-type peptidase activity	3,6	
	fucosyltransferase activity	12,8	
	endopeptidase activity	2,4	3,9
	nucleotide receptor activity	8,7	
	purinergic nucleotide receptor activity	8,7	
	cytokine receptor activity	8,0	
	lipid binding	2,7	
	voltage-gated chloride channel activity	12,1	
	metalloendopeptidase activity		9,2
GO:Cellular Component	MHC class II protein complex	7,5	
	vacuole	6,2	

*Ensembl ID codes of the significantly enriched genes in eGFP-positive macrophages from *mpeg1:egfp* transgenic zebrafish (mpeg1+) or in eGFP-positive neutrophils from *mpx:egfp* transgenic zebrafish (mpx+) were analyzed using DAVID. The table shows the fold enrichment of KEGG pathways and GO terms for Biological Process, Molecular Function, and Cellular Component in the eGFP-positive cell fractions with a false discovery rate of less than 5%.

Comparison of macrophage, neutrophil, and early T-cell gene signatures

In addition to the *mpeg1:egfp* line for macrophages, we used *mpx:egfp* and *lck:egfp* transgenic lines for FACS sorting and RNA-Seq analysis of neutrophil and early T-cell populations. First, we looked at the expression levels of several marker genes that are commonly used to identify different leukocyte and lymphoid subpopulations in

zebrafish (Table 2). As expected, *mpeg1*, *mpx*, and *lck* RPKM values (read count per kilobase per million mapped reads) were highest in the eGFP-positive cell fractions of macrophages, neutrophils, and T-cells, respectively. Other macrophage markers, including *csf1r*, *cxcr3.2*, *irf8*, *marco*, *mfap4*, and *mhc2dab* were also enriched in *mpeg1:egfp*-positive cells. Among all macrophage markers, *mfap4* showed the highest expression level, and *mhc2dab* showed the highest specificity, with an over 60-fold higher RPKM value than in *mpx:egfp*-positive neutophils. In addition to *mpx*, neutrophils showed higher expression of *lyz*, *mmp9* and *mmp13a* than macrophages. The *lck:egfp*-positive cell fraction showed highly specific expression of T-cell markers, which apart from *lck* included *cd2*, *cd28*, *cd4*, *ikzf1* (*ikaros*), *rag1*, and *rag2*. However, expression of *cd8* was not detectable, suggesting that cytotoxic T-cell activity is not yet present at 5 dpf. Finally, the hematopoietic transcription factor gene *spi1* was specific for the myeloid cell fractions, while *coro1a*, *lcp1* (*L-plastin*), *ptprc* (*cd45*), and *ptpn6* were commonly expressed in myeloid and lymphoid cells.

More than 70% of all 283 genes that were significantly enriched in *mpx:egfp*-positive neutrophils compared to the eGFP-negative background were also significantly enriched in *mpeg1:egfp*-positive macrophages (Fig. 1). In contrast, only 11% of all 2578 genes enriched in *lck:egfp*-positive T-cells were also enriched in either one or both of the myeloid cell fractions (Fig. 1). Next, we searched for genes in the *mpeg1:egfp* gene set with higher expression level or better macrophage specificity than *mpeg1*, which had an RPKM of 126 in *mpeg:egfp*-positive cells and 12 in *mpx:egfp*-positive cells. Genes with higher abundance than *mpeg1* belonged to the families of chemokines, immunoglobulins, olfactomedins, granulins, cathepsins, fibrinogens (*mfap4* and 2 paralogues), lectins, transmebrane receptors, complement factors (C1q), MHC II class proteins, and also included some predicted non-coding RNAs (Table 3A). Among these, the most specific marker for macrophages was *granulin 2* (*grn2*), which was expressed at over 10-fold higher level than *mpeg1* and showed an approximately 300-fold higher RPKM in macrophages than in the neutrophil or T-cell fractions. Other highly specific macrophage markers were the immunoglobulin gene *dicp1*.1, the transmembrane receptor gene *ocstamp*, and MHC class II genes, like *cd74* and *mhc2dab*. In neutrophils, the lysozyme (*lyz*) and nephrosin (*npsn*) genes were expressed at approximately 28- and 4-fold higher level, respectively, than *mpx* (Table 3B). However, the specificity of *mpx* (17-fold higher RPKM than in macrophages) was better than that of *lyz* (12-fold higher) and npsn (8-fold higher). In addition, interleukin 34 (*il34* (1 of 2)) also showed high neutrophil specificity (21-fold higher RPKM than in macrophages), but its expression level was 4-fold lower than that of *mpx*. Markers for T-cells expressed at higher or similar level as *lck* were all highly specific for lymphoid cells and barely or not detectable in myeloid cells (Table 4). These markers included for example *rag1*, cytokine receptor genes (*ccr9b*, *il17r*), various other receptor genes (T-cell-specific immunoglobulins, a member of the signaling lymphocyte activation (SLAM)-family, *p2rx1*, *rorc*), and the transcription factor gene *foxp3a*. In conclusion, our RNA-Seq analysis identified several abundant and specific markers for macrophages, neutrophils,

and T-cells, that are good candidates for developing new transgenic lines and antibodies for distinguishing leukocyte lineages in the zebrafish model.

Table 2. Expression levels of commonly used lineage markers for different leukocyte cell types*

Lineage specificity	Gene symbol	Ensembl ID	mpeg1+	mpx+	lck+	GFP-
macrophage-enriched	*csf1ra*	ENSDARG00000007889	9	3	0	1
	cxcr3.2	ENSDARG00000041041	62	26	0	3
	irf8	ENSDARG00000056407	25	9	0	3
	marco	ENSDARG00000059294	4	0	0	0
	mfap4	ENSDARG00000090783	980	130	3	14
	mhc2dab	ENSDARG00000079105	192	3	0	1
	mpeg1	ENSDARG00000055290	126	12	0	5
neutrophil-enriched	*lyz*	ENSDARG00000057789	1461	18294	0	64
	mpx	ENSDARG00000019521	37	662	0	2
	mmp9	ENSDARG00000042816	357	1341	15	34
	mmp13a	ENSDARG00000012395	320	638	5	13
common myeloid	*spi1*	ENSDARG00000000767	340	253	1	7
lymphoid	*cd2*	ENSDARG00000091109	0	0	31	1
	cd28	ENSDARG00000095070	3	8	14	2
	cd4	ENSDARG00000070668	0	0	27	1
	ikzf1	ENSDARG00000013539	5	5	24	2
	lck	ENSDARG00000059282	1	0	237	3
	rag1	ENSDARG00000052122	0	0	409	11
	rag2	ENSDARG00000052121	0	0	48	2
common leukocyte	*coro1a*	ENSDARG00000054610	164	170	197	19
	lcp1	ENSDARG00000023188	63	92	14	10
	ptprc	ENSDARG00000071437	49	54	23	3
	ptpn6	ENSDARG00000089043/ ENSDARG00000013916	82	97	25	8

*RNA-Seq libraries were prepared from eGFP-positive (+) and negative (-) cell fractions obtained by dissociating and FACS-sorting 5-6 dpf larvae of transgenic lines expressing enhanced GFP under control of the mpeg1, mpx, or lck promoters. RPKM values (read counts per kilobase per million mapped reads) are averaged from 4 biological replicates of eGFP-positive cells from mpeg1:egfp larvae (mpeg1+, 2x 5dpf, 2x 6 dpf), 3 biological replicates from mpx:egfp larvae (mpx+, 5 dpf), and 2 biological replicates from lck:egfp larvae (lck+, 5 dpf). The RPKM value for eGFP-negative cells is the average of all libraries. Enriched expression in macrophages, neutrophils, or T-lymphoblasts is indicated in orange, green, and blue, respectively. RPKM values in the range of 10-50, 50-100, 100-200, 200-500, and over 500 are shown with increasingly darker shades of color. Genes classified as macrophage-enriched have at least 2-fold higher expression than in neutrophils, and genes classified as neutrophil-enriched have at least 2-fold higher expression than in macrophages.

Table 3. Myeloid-specific markers*

Gene symbol	Annotation group	Ensembl ID	mpeg1+	mpx+	lck+	GFP-
A. Macrophage markers						
si:ch211-149o7.4	chemokines (interleukin8-like)	ENSDARG00000079736	5852	245	316	91
si:ch211-149p10.2	immunoglobulin v-set family	ENSDARG00000079553	2633	422	95	86
si:dkey-25o1.6	chemokines (interleukin8-like)	ENSDARG00000093608	2002	60	7	22
CR384059.2	olfactomedin glycoprotein family	ENSDARG00000086947	1646	183	1	16
CR384059.1	olfactomedin glycoprotein family	ENSDARG00000074322	1552	166	0	15
grn2	growth factors	ENSDARG00000088641	1294	5	4	3
si:ch211-122l24.4	chemokines (interleukin8-like)	ENSDARG00000090873	1265	101	0	11
ctsl.1	cathepsin protease family	ENSDARG00000003902	1119	91	1	14
zgc:173915	fibrinogen family (paralogue of mfap4)	ENSDARG00000088745	1108	82	2	17
DKEY-119G10.5	long intervening non-coding RNA	ENSDARG00000087623	996	42	18	7
mfap4	fibrinogen family	ENSDARG00000090783	980	130	3	14
vmp1	endomembrane system	ENSDARG00000012450	642	52	18	18
havcr1	immunoglobulin v-set family receptor	ENSDARG00000040178	571	46	3	8
lgals2a	lectins	ENSDARG00000054942	535	82	3	14
lygl1	glycoside hydrolases	ENSDARG00000056874	484	82	7	9
DKEY-119G10.4	long intervening non-coding RNA	ENSDARG00000095801	438	70	0	3
si:dkey-5n18.1	C1q complement family	ENSDARG00000043436	435	34	3	4
DKEY-6N3.3	long intervening non-coding RNA	ENSDARG00000095820	427	24	0	2
si:ch1073-403i13.1	MHC class II	ENSDARG00000001832	422	29	4	6
cd74	MHC class II	ENSDARG00000036628	346	6	20	5
cd74a	MHC class II	ENSDARG00000009087	277	12	8	3
ocstamp	transmembrane receptor	ENSDARG00000022139	237	3	0	2
mhc2dab	MHC class II	ENSDARG00000079105	192	3	0	1
zgc:194314	lipid metabolism	ENSDARG00000078859	189	24	3	5
si:dkey-15g19.2	non-coding RNA	ENSDARG00000095693	169	4	2	6
si:zfos-2330d3.3	fibrinogen family (paralogue of mfap4)	ENSDARG00000089667	161	7	4	2
rnaset2l	ribonuclease T2 family	ENSDARG00000058413	145	6	0	2
BX649485.1	immunoglobulin v-set family	ENSDARG00000089473	145	26	6	1
CABZ01074899.1	gamma-glutamyl hydrolase	ENSDARG00000025237	142	25	0	3

grn1	growth factors	ENSDARG00000089362	140	16	3	2
mpeg1	membrane attack complex	ENSDARG00000055290	126	12	0	5
sftpb (2 of 2)	surfactant proteins	ENSDARG00000067566	118	14	6	5
dicp1.1	immunoglobulin family	ENSDARG00000091993	109	1	3	4
ctssb.2	cathepsin protease family	ENSDARG00000013771	109	14	0	2
si:dkeyp-2h4.2	MHC class II	ENSDARG00000031745	103	3	2	3
B. Neutrophil markers						
lyz	glycoside hydrolases	ENSDARG00000057789	1461	18294	0	64
npsn	metalloendopeptidases	ENSDARG00000010423	266	2347	0	7
mpx	peroxidases	ENSDARG00000019521	37	662	0	2
si:dkey-238m4.4	unknown	ENSDARG00000093248	66	454	0	1
sult2st1	sulfate transferases	ENSDARG00000086446	31	375	4	7
alox5ap	leukotriene biosynthesis	ENSDARG00000054755	49	294	0	3
CU682604.2	lamin B receptor family	ENSDARG00000075664	15	224	0	3
il6r	cytokine receptors	ENSDARG00000070398	21	188	0	3
il34 (1 of 2)	cytokines	ENSDARG00000091003	8	171	1	3
il34 (2 of 2)	cytokines	ENSDARG00000069128	21	152	10	7
sult2st1	sulfate transferases	ENSDARG00000033170	15	118	2	5

*Macrophage-specific genes (A) were selected based on significantly enriched expression in mpeg1:egfp-positive cells (mpeg1+, log2 fold change > 2, adjusted P-value <0.1), a minimum RPKM value of 100, and >5-fold higher RPKM than in mpx:egfp-positive cells (mpx+), >10-fold higher RPKM than in lck:egfp-positive cells (lck+), and >20-fold higher RPKM than in eGFP-negative cells. Neutrophil-specific genes (B) were selected based on significantly enriched expression in mpx:egfp-positive cells (log2 fold change > 2, adjusted P-value <0.1), a minimum RPKM value of 100, and >5-fold higher RPKM than in mpeg1:egfp-positive cells, >10-fold higher RPKM than in lck:egfp-positive cells, and >20-fold higher RPKM than in gfp-negative cells. RNA-Seq library preparation, averaging of RPKM values from biological replicates, and the use of increasingly darker shades of different colors to indicate higher expression levels were as in Table 2. The full lists of significantly enriched genes in mpeg1:egfp-positive and mpx:egfp-positive cells with fold change and P-value are given in Supplementary Table 2.

Table 4. Lymphoid-specific markers*

Gene symbol	Annotation group	Ensembl ID	mpeg1+	mpx+	lck+	GFP-
CT867973.1	T-cell receptor immunoglobulin family	ENSDARG00000075807	1	0	1718	19
ccr9b	cytokine receptors	ENSDARG00000068310	0	0	664	5
CT583625.4	immunoglobulin V-set domain	ENSDARG00000094770	3	2	650	4
rag1	recombination	ENSDARG00000052122	0	0	409	11
zgc:171686	signaling lymphocyte activation molecule (SLAM)-family receptors	ENSDARG00000076721	1	2	406	6
p2rx1	ion-gated receptor family	ENSDARG00000016695	3	1	276	8
lck	tyrosine kinase family	ENSDARG00000059282	1	0	237	3
ms4a17c.1	membrane proteins	ENSDARG00000094643	1	0	196	3
BX323450.2	sphingolipid activator protein (saposin) family	ENSDARG00000058673	1	1	192	3
rorc	nuclear receptor superfamily	ENSDARG00000087195	0	0	155	4
plp2 (2 of 2)	endomembrane system	ENSDARG00000042972	1	0	140	5
foxp3a	transcription factors	ENSDARG00000055750	0	0	138	1
si:ch211-132g1.1	non-coding RNA	ENSDARG00000040250	6	0	132	2
sh2d1a (1 of 2)	SH2-domain family	ENSDARG00000074854	2	2	123	2
rhoh	ras family	ENSDARG00000070121	0	2	116	1
il7r	cytokine receptors	ENSDARG00000078970	5	3	103	3

*Genes specific for early T-lymphocytes in zebrafish larvae were selected based on significantly enriched expression in lck:egfp-positive cells (lck+, log2 fold change > 2, adjusted P-value <0.1), a minimum RPKM value of 100, and >10-fold higher RPKM than in mpeg1:egfp-positive cells (mpeg1+), >10-fold higher RPKM than in mpx:egfp-positive cells (mpx+), and >20-fold higher expression than in gfp-negative cells. RNA-Seq library preparation, averaging of RPKM values from biological replicates, and the use of increasingly darker shades of different colors to indicate higher expression levels were as in Table 2. The full list of significantly enriched genes in lck:egfp-positive cells with fold change and P-value is given in Supplementary Table 2.

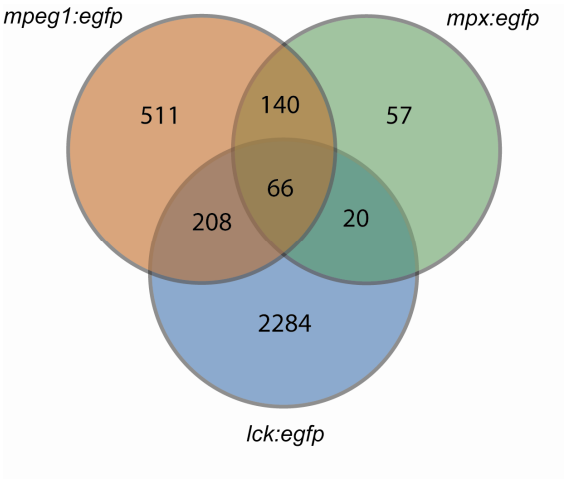

Figure 1. Overlap between genes enriched in GFP-positive cell fractions from mpeg1:egfp, mpx:egfp, and lck:egfp larvae. RNA-Seq libraries were prepared from GFP-positive (+) and negative (-) cell fractions obtained by dissociating and FACS-sorting 5-6 dpf larvae of transgenic lines expressing enhanced GFP under control of the mpeg1, mpx, or lck promoters. DESeq analysis was used to compare the read count data of the GFP-positive versus the GFP-negative cell fractions with 4 biological replicates of mpeg1:egfp larvae (2x 5dpf, 2x 6 dpf), 3 biological replicates of mpx:egfp larvae (5 dpf), and 2 biological replicates of lck:egfp larvae (5 dpf). The Venn-diagram shows the overlap between genes enriched in the GFP-postive cell fractions of the different transgenic lines (log2 fold change >2 and adjusted P-value <0.1).

Expression profile of *M. marinum*-infected cells

The mycobacterium genus comprises several intracellular pathogens that reside in macrophages, including the human pathogen *Mycobacterium tuberculosis* and the fish pathogen *M. marinum*. The hallmark of infectious diseases caused by *M. tuberculosis* or *M. marinum* is that infected macrophages are manipulated to attract uninfected macrophages and other immune cells to form tissue aggregates, known as tuberculous granulomas. These granulomas form a niche for the chronic persistence of mycobacteria inside their host. Zebrafish embryos are a well-characterized model to study the early stages of *M. marinum*-macrophage interaction and granuloma formation (Davis et al., 2002, Ramakrishnan, 2012). To investigate the effect of *M. marinum* on gene expression in macrophages, we infected 1-day-old embryos with mCherry-labeled *M. marinum* Mma20 bacteria and isolated the infected cells by FACS sorting at 4 days post infection (dpi) when early stage granulomas are formed. We compared the RNA-Seq profile of the Mma20-infected cells to the eGFP-negative background from uninfected *mpeg1:egfp* larvae, and investigated the overlap between Mma20-positive cells and eGFP-positive macrophages from uninfected *mpeg1:egfp* larvae (Fig. 2). This comparison showed that out of 188 genes enriched in Mma20-infected cells (Supplementary Table 3), only 40 were overlapping with the gene set of uninfected macrophages. The overlapping genes included some of the most specific macrophage

markers that we described above, such as *grn2* and the MHC class II gene *cd74*. Expression of *mfap4* and two *mfap4* paralogues was also detected, however, *mpeg1* was notably absent. Furthermore, the majority of the 40 macrophage-specific genes were expressed at over 10-fold lower levels in Mma20-infected cells compared with uninfected macrophages. One possible explanation could be that only a small portion of the Mma20-infected cell population consists of macrophages. However, this is very unlikely, because it has been well described that *M. marinum* is rapidly phagocytosed by macrophages after injection of bacteria into the blood circulation, and that the infection spreads to newly attracted macrophages, which phagocytose infected macrophages undergoing apoptosis (Davis and Ramakrishnan., 2009). Furthermore, a preliminary RNA-Seq analysis of red/green double fluorescent *mpeg1:egfp*-cells infected with mCherry-labelled Mma20 also shows strong down-regulation of macrophage markers (data not shown). Therefore, the down-regulation of macrophage markers is more likely due to *M. marinum*-induced transformation of infected macrophages . Indeed, it is well known that infected macrophages in tuberculous granulomas are manipulated to adopt epithelial and multinucleate morphologies (Russell, 2011) and such morphological changes have also been observed in the granulomas of zebrafish larvae (Davis et al., 2002).

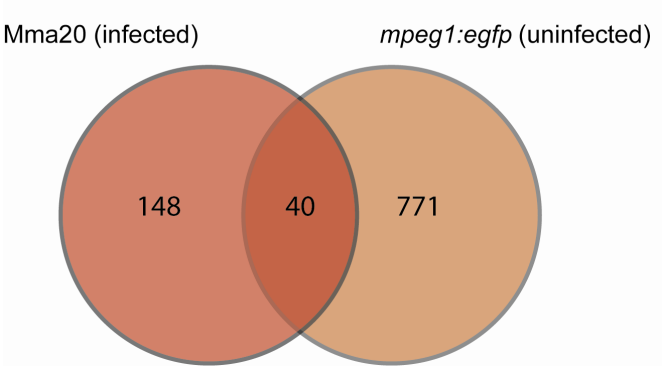

Figure 2. Overlap between genes enriched in M. marinum-infected cells and genes enriched in macrophages. Embryos were infected by intravenous injection of mCherry-labeled *M. marinum* Mma20 bacteria at 1 dpf, and at 4 dpi (5dpf) RNA-Seq libraries were prepared from mCherry-positive and negative cell fractions obtained by FACS-sorting. Read counts of the mCherry-positive fraction from two biological replicates of infected embryos were compared by DESeq analysis against the GFP-negative cell fractions of two biological replicates of uninfected *mpeg1:egfp* larvae (5 dpf). The Venn-diagram shows the overlap of genes enriched in Mma20-infected cells with genes enriched in *mpeg1:efgp*-positive macrophages from two biological replicates of uninfected larvae (log2 fold change >2 and adjusted Pvalue <0.1.

The genes enriched in Mma20-infected cells that did not overlap with macrophage markers (148 out of 188 genes) were analyzed using DAVID, which identified five enriched clusters of GO-terms: ribosome, oxidative phosphorylation, proteolysis, ion transport, and chromatin assembly (Supplementary Table 4). This enrichment may reflect activation of protein translation and defense mechanisms in the

infected cells. For example, the ion transport cluster contained the antimicrobial hepcidin gene (*hamp1*), and it has recently emerged that ribosomal protein genes, such as *rps3* which was up-regulated, have extra-ribosomal regulatory functions in the innate immune system (Gao and Hardwidge, 2011). It is an interesting possibility, warranting further investigation, that the increased expression of genes involved in chromatin assembly might be associated with the mycobacterium-induced morphological changes in macrophages or suppression of the macrophage immune defenses. By manual inspection of the gene list we defined three additional annotation clusters. The first consisted of genes involved in lipid metabolism and transport. An elevation of host lipid metabolism has also been observed in microarray analysis of caseating human tuberculous granulomas (Kim et al., 2010). The second cluster was a group of lectin genes, including members of the galactoside-binding lectin family, which in human macrophages have been shown to accumulate around mycobacterium-containing phagosomes (Beatty et al., 2002), and a member of the mannose-binding lectins, associated with human tuberculosis susceptibility (Denholm et al., 2010; Singla et al., 2012). Finally, the third cluster consisted of a group of three genes for immunosuppressive proteins, including two FK506-binding proteins and a vasointestinal peptide, which has been implicated in switching off activated macrophages during *M. tuberculosis* infection (Ma et al., 2003; Souza-Moreira et al., 2011). In conclusion, our analysis of *M. marinum*-infected cells showed a general down-regulation of macrophage marker genes accompanied by the induction of several specific gene groups that may be linked to processes of host defense and to the immunosuppressive effects of mycobacteria on host cells.

Ptpn6 knockdown effect on expression profiles of leukocyte populations and *M. marinum*-infected cells

Ptpn6, also known as Shp-1, is a hematopoietic SH2-domain containing non-receptor type protein tyrosine phosphatase and a well-known negative regulator of innate and adaptive immune responses in human and mice (Blanchette et al., 2009; Kumagai et al., 2012; Henshall et al., 2001; Oh et al., 2009). We have previously shown that morpholino knockdown of *ptpn6* in zebrafish leads to increased susceptibility to *M. marinum* infection (Chapter 2). In addition, uninfected *ptpn6* morphants developed an inflammation-associated phenotype at the late larval stage (Chapter 2). RNA-Seq analysis demonstrated *ptpn6* expression in both myeloid and lymphoid cells (Table 2), in agreement with previous in situ hybridization results (Zakrzewska et al., 2010). To gain a better understanding of the underlying causes of the *ptpn6* morpholino knockdown effects, we performed RNA-Seq analysis on FACS-sorted leukocyte populations from *ptpn6* morphants and controls at 5 dpf, including *M. marinum*-infected cells, macrophages, neutrophils and T-cells. In addition, we analyzed the eGFP-negative background from uninfected *mpeg1:egfp* larvae. The results of all comparisons are summarized in Table 5 and details of expression levels are given in Supplementary Table 5.

In agreement with previous qPCR analysis (Chapter 2), RNA-Seq analysis revealed increased *mmp9* expression in *ptpn6* morphants. Notably, in Mma20-infected cells from *ptpn6* morphants not only *mmp9*, but also *mmp2*, *mmp13a* and the *mmp* (matrix metalloproteinase) inhibitor gene *timp2b* were increased compared with infected cells of control embryos. The *mmp9* and *mmp13a* genes were also specifically up-regulated in macrophages from *ptpn6* morphants, while *mmp2* was also up-regulated in neutrophils and in the eGFP-negative background of *ptpn6* morphants. There was no general up-regulation of pro-inflammatory genes in any of the *ptpn6* morphant cell types. Therefore, the effect of *ptpn6* knockdown on the immune response of zebrafish embryos towards *M. marinum* infection is markedly different from the effect of *ptpn6* knockdown during *S. typhimurium* infection, where the up-regulation of *mmp9* and *mmp13a* genes goes together with a general up-regulation of pro-inflammatory cytokines and immune-related transcription factors (Chapter 2).

In addition to the up-regulation of *mmp* pathway genes, Mma20-infected cells of *ptpn6* morphants showed strongly increased expression of *serum amyloid A* (*saa*). This apolipoprotein family gene encodes a major acute phase protein that is known to be highly expressed in response to inflammation and tissue injury. Interestingly, several reports have suggested a link between expression of *saa* and *mmp* genes, which may also underlie connection between chronic inflammation and cancer (Malle et al., 2009). Transcription of *MMP9* was found to be induced by SAA in human monocytic cells via the formyl methionine receptor (Lee et al., 2005). Furthermore, an SAA-activating factor (SAF-1) was shown to function cooperatively with the AP-1 transcription factor complex to activate *MMP9* transcription (Ray et al., 2005). SAA has also been linked to granulomatous inflammation (Chen et al., 2010). Increased expression of *mmp9* has been shown to be essential for granuloma formation in zebrafish embryos (Volkman et al., 2010). In this study, *mmp9* secretion by epithelial cells nearby granulomas was proposed to drive macrophage recruitment. Our RNA-Seq data do not exclude *mmp9* expression by epithelial cells, but do show that the major induction of *mmp9* occurs directly in Mma20-infected cells and is enhanced by *ptpn6* knockdown together with a strong induction of *mmp13a* in these cells. As granuloma formation is accelerated in *ptpn6* morphants, we propose that Saa-dependent induction of *mmp9* and *mmp13a* in Mma20-infected cells plays a major role in the formation and expansion of granulomas (Fig. 3).

Another gene that showed increased up-regulated in Mma20-infected cells under *ptpn6* knockdown conditions was *hamp1*, and a *ptpn6*-dependent increase of *hamp1* expression was also observed in *lck:egfp*-positive T-cells and in eGFP-negative background cells. Hepcidin, the product of *hamp1*, regulates iron homeostasis by mediating the degradation of the iron export protein ferroportin 1, and is known to inhibit growth of *M. tuberculosis* (Sow et al., 2007, Sow et al., 2011). Three other genes connected with responses to nutrients also showed increased up-regulation in Mma20-infected cells of *ptpn6* morphants. These included the genes for the peptide hormones leptin b (*lepb*) and glucagon a (*gcga*) and the *steap4* gene, which encodes a plasma membrane metalloreductase involved in iron and copper transport. Leptin b has been

suggested to play a role in the early immune response to pulmonary tuberculosis, and mice deficient in leptin b or in the leptin receptor displayed disorganized granulomas (Wieland et al., 2005, Lemos et al., 2011). The *steap* 4 gene is homologous to the human tumor necrosis factor alpha-induced protein 9 gene (*TNFAIP9*, also known as *STEAP4* or *STAMP2*), which has been proposed to play an important role in integrating inflammatory and metabolic responses and to act as an anti-inflammatory protein in macrophages (Wellen et al., 2007; Ten Freyhaus et al., 2012). We have previously shown that that an alternative splice variant of this gene is induced by *M. marinum* infection in adult zebrafish (Hegedus et al., 2009). Any possible antimicrobial effects of *hamp1*, *lepb*, *gcga* or *steap4* were not sufficient to prevent increased *M. marinum* Mma20 infection in *ptpn6* morphants.

Knockdown of *ptpn6* also led to down-regulation of genes in Mma20-infected cells in comparison with infected cells of control embryos, for example, a chemokine gene (*si:ch211-149o7.4*) and the chemokine receptor gene *cxcr4b*. Both these genes are highly expressed in macrophages and other immune cell types of zebrafish larvae (Table 3, Supplementary Table 2). As we have shown that *M. marinum* infection lead to a general down-regulation of macrophage markers, the down-regulation of *si:ch211-149o7.4* and *cxcr4b* might reflect the advanced stage of infection in *ptpn6* morphants. Both genes were also down-regulated in macrophages of uninfected *ptpn6* morphants, along with other macrophage-expressed genes, such as *tnfa*, *tnfrsf1a*, *mbp*, *grn2*, *mhc2dab*, *cd74* and *cd74a*. In contrast, *ptpn6* knockdown in uninfected macrophages led to up-regulation of among others actin, myosin and parvalbumin genes, several immune-related proteases (*cpa5*, *npsn*, *cpn1* in addition to the *mmp9* and *mmp13a* genes discussed above), and of typical neutrophil markers like *lyz* and *mpx*. These data suggest a complex role of *ptpn6* in regulating the activation status of macrophages.

Under uninfected conditions, the *ptpn6* knockdown effects on different cell populations were very specific. The up-regulation of *mmp* and other protease genes was observed in *ptpn6*-deficient macrophages but not in *ptpn6*-deficient neutrophils or T-cells. An up-regulation of genes involved in p53 signaling (*tp53*, *mdm2*, *ccng1*) was only observed in *ptpn6*-deficient neutrophils. Furthermore, neutrophils showed specific down-regulation of apolipoprotein and protease genes under *ptpn6* knockdown conditions, while down-regulation of ribosomal protein genes was specific for T-cells. There was no effect on p53 signaling genes in the eGFP-negative background cells of *ptpn6* morphants and no indication of a general toxicity effect in the RNA-Seq data. Therefore, enhanced *mmp* genes secretion by macrophages might be a major cause of the inflammation-associated phenotype that develops at the late larval stage in *ptpn6* morphants.

Table 5. Effect of *ptpn6* knockdown on gene expression in M. marinum-infected cells and different leukocyte populations*

	ptpn6 MO1 up-regulated					ptpn6 MO1 down-regulated				
	Mma20 +	mpeg1 +	mpx +	lck +	GFP -	Mma20 +	mpeg1 +	mpx +	lck +	GFP -
Total no. of genes	22	58	23	39	88	38	40	25	12	37
Matrix metalloproteinases/ inhibitors										
mmp2	√		√		√					
mmp9, mmp13a	√	√								
timp2b	√									
Other proteases										
try					√			√		
cpa5		√			√					
npsn, cpn1		√								
cela1, cpb1, ela2, cpa4								√		
adamts1					√					
Iron transport										
hamp1	√			√	√					
steap4	√				√					
tfa						√				√
hbm						√				
Peptide hormones										
lepb	√			√						
gcga	√									
prl, adm					√					
lepa				√						
Acute phase proteins										
saa	√									
apcs						√				
Apolipoproteins					√					
apom, apoc2						√				
apoc1l						√		√		
apoa2								√	√	√
apod (3 of 3)					√			√		
Actin/myosin/tropomyosin										
tnnc2, myl3		√								
mylz2		√		√	√					
mylz3, tnni2a.4		√			√					
acta2	√									
acta1a, acta1b, actc1b, myhz1.1, myl10, tnnc1b, tnni2b.2, tnnt3b		√								

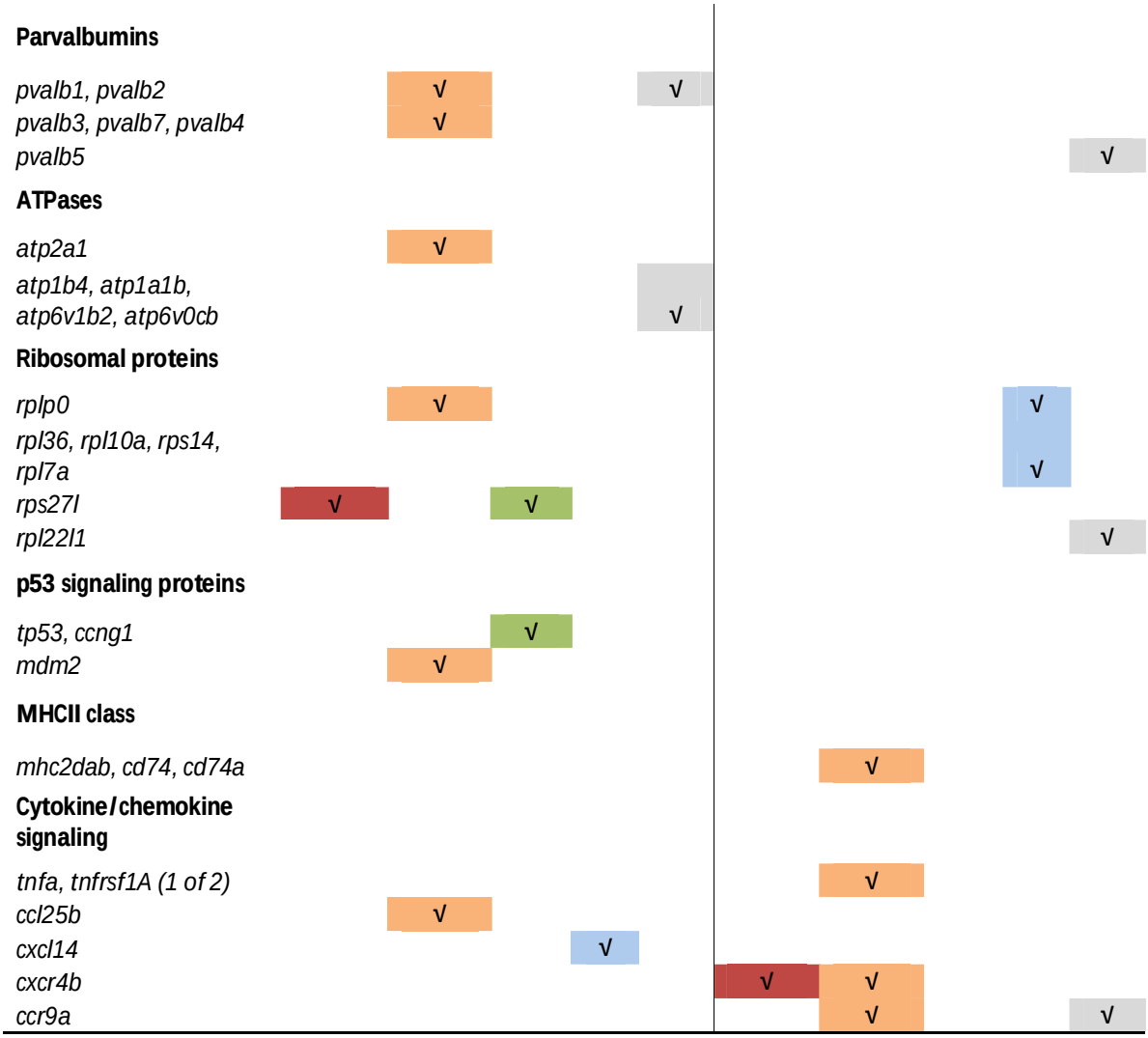

*Embryos injected with a morpholino against ptpn6 (ptpn6 MO1) or control embryos were infected with mCherry-labelled M. marinum Mma20 bacteria at 1 dpf and RNA-Seq libraries were prepared from mCherry-positive (+) and negative (-) cell fractions at 4 dpi (5 dpf) as in Supplementary Table 4. Likewise, ptpn6 MO1 was injected in embryos from mpeg1:egfp, mpx:egfp, and lck:egfp transgenic embryos to compare macrophage (mpeg1+), neutrophil (mpx+), and T-lymphoblast (lck+) expression levels at 5 dpf with those from control larvae. The eGFP-negative cell fractions from mpeg1:egfp larvae were used to determine the effect of ptpn6 MO1 on gene expression levels in the background without macrophages. Two biological replicates were used for all comparisons. Genes are ordered by annotation groups to show up- or down-regulation by ptpn6 MO1 in the different cell fractions. Significance cut-offs in DESeq analysis were log2 fold change >2 and P <0.1. As an additional criterion, genes up-regulated by ptpn6 MO1 showed a minimum RPKM of 30 in both replicates of the respective ptpn6 MO1 groups of each FACS-sorting, and genes down-regulated by ptpn6 MO1 showed a minimum RPKM of 30 in both replicates of the respective control groups. The full list of up- or down-regulated genes with fold change, P-value, and RPKM values of the biological replicates in given in Supplementary table 5.

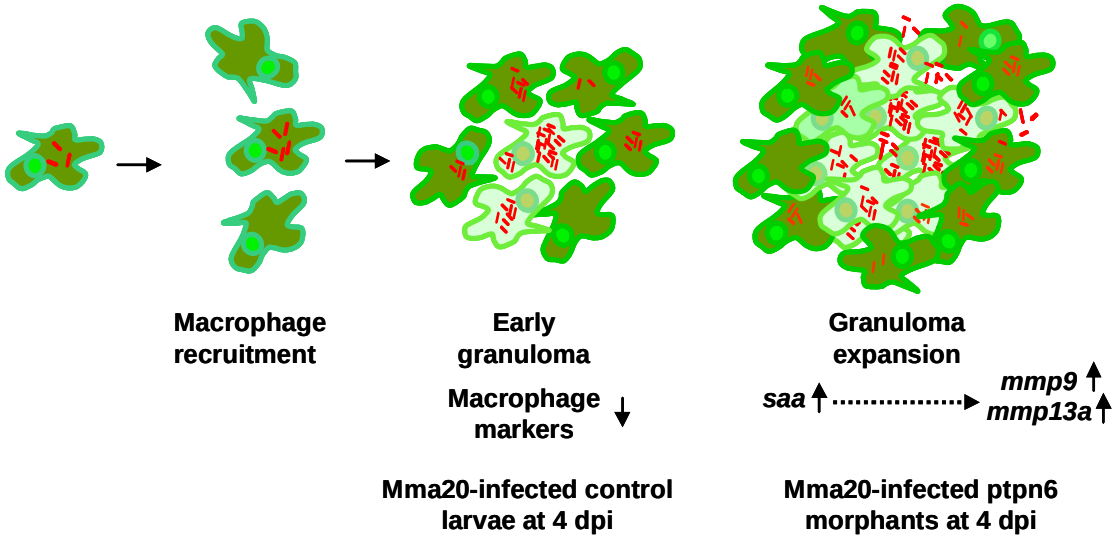

Figure 3. Model for granuloma expansion in wild type zebrafish larvae and ptpn6 morphants. Intravenously injected *M. marinum* bacteria are rapidly phagocytosed by embryonic macrophages in the blood circulation of 1 day-old embryos. Infected macrophages migrate into tissue and attract other uninfected macrophages to form granuloma-like aggregates (Davis et al., 2002). These early stages of granulomas are exploited by mycobacteria for spreading to other macrophages that facilitate tissue dissemination of the infection (Clay et al., 2007, Davis et al., 2009) and granuloma formation has been shown to require the function of *mmp9* (Volkman et al., 2010). In this study we show that the expression of macrophage marker genes is down-regulated upon proliferation of *M. marinum* inside these cells (indicated by a lighter color green of macrophages in the figure). As the infection progresses, infected cells up-regulate expression of serum amyloid A (saa) and matrix metalloproteinase (*mmp*) genes. Up-regulation of *mmp9* and *mmp13a* is proposed to be regulated by *saa*. Under conditions of *ptpn6* morpholino knockdown an increased bacterial burden and size of granuloma-like aggregates is observed. In the present study, *ptpn6* morphants showed increased expression of *saa*, *mmp9*, and *mmp13a* at 4 days post infection compared to control infected larvae, which had smaller granulomas that were not yet at the advanced stage of development where these genes are up-regulated.

Conclusions

By means of RNA-Seq analysis of FACS-sorted leukocyte and lymphoid subpopulations from fluorescent reporter lines we could determine gene expression signatures of macrophages, neutrophils and early T-cells in zebrafish larvae. Commonly used markers, including *mpeg1* for macrophages, *mpx* for neutrophils, and *lck* for T-cells, faithfully distinguished the different leukocyte subtypes in the RNA-Seq data. In addition, our RNA-Seq analysis identified other more abundant or more specific markers for macrophages, neutrophils, and T-cells, which will be highly useful for developing new reporter lines and lineage-specific antibodies for zebrafish. For example, the granulin gene *grn2* was highly abundant and almost exclusively detectable in macrophages, whereas *mpeg1* expression showed some overlap with neutrophils and was expressed at 10-fold lower level than *grn2*. MHC class II genes were also highly

specific for macrophages. The macrophage gene signature was markedly changed by *M. marinum* infection. This infection led to a general down-regulation of macrophage marker genes accompanied by an induction of ribosomal protein genes and genes involved in oxidative phosphorylation, proteolysis, transport of iron and other ions, chromatin assembly, lipid metabolism, carbohydrate binding, and immunosuppression. Knockdown of the protein tyrosine phosphatase gene *ptpn6*, which is known as a negative regulator of immune responses, also had specific effects on the macrophage expression profile of zebrafish larvae. Notably, expression of matrix metalloproteinase genes *mmp9* and *mmp13a* was specifically up-regulated in *ptpn6*-deficient macrophages. Likewise, these matrix metalloproteinase genes were also strongly up-regulated in *M. marinum*-infected cells of *ptpn6* morphants, along with the expression of the serum amyloid A gene (*saa*), which has been implicated in regulating matrix metalloproteinase gene expression. The induction of these genes at high levels in *M. marinum*-infected cells is not beneficial to the host, as the bacterial burden is strongly enhanced in *ptpn6* morphants. Increased expression of these genes in infected *ptpn6*-deficient macrophages may accelerate the formation of granulomas, which are exploited by mycobacteria for their expansion and tissue dissemination (Fig. 3).

Acknowledgements

We thank Guido de Roo (Leiden University Medical Center, The Netherlands) for expert advice and help with FACS sorting. Furthermore, we thank Ulrike Nehrdich and Davy de Witt for fish care, and members of the molecular cell biology group for helpful discussions. ZK was supported by a fellowship of the Higher Education Commission of Pakistan, and AZ was supported by a Horizon grant of the Netherlands Genomics Initiative. This work was further supported by the Smart Mix Program of The Netherlands Ministry of Economic Affairs and the Ministry of Education, Culture and Science, and by the European Commission 7th framework programme, under the project ZF-HEALTH (HEALTH-F4-2010-242048) and the European Marie-Curie Initial Training Network FishForPharma (PITN-GA-2011-289209).

Supplementary data

Supplementary Table 1. Overlap in significant genes in biological replicates of FACS-sorted macrophages from mpeg1:egfp transgenic embryos*

replicates	#2	#3	#4
#1	51%	42%	68%
#2		47%	62%
#3			56%

*Four independent pools of approximately 250 5-day-old (#1, #2) or 6-day-old (#3, #4) larvae from *mpeg1:egfp* transgenic zebrafish were subjected to FACS-sorting on different days. For each replicate the eGFP-positive cell fraction was compared against the eGFP-negative background by DESeq analysis to determine the number of genes showing significant enrichment in eGFP-positive macrophages. The overlap in significant genes between replicates is shown as the percentage of the total number of genes in the smaller group of the replicate pair.

Supplementary Table 2. Genes enriched in eGFP-positive cell fractions from mpeg1:egfp, mpx:egfp, and lck:egfp larvae. Supplementary table can be found online at: https://www.dropbox.com/s/g06wjz5zqm324xn/Chapter3suppl.table2.xlsx

Supplementary Table 3. Overview of 148 genes enriched in *M. marinum*-infected cells. Supplementary table can be found online at: https://www.dropbox.com/s/zp95a6c8v2mes9w/Chapter3suppl.table3.xlsx

Supplementary Table 4. Genes enriched in *M. marinum*-infected cells*

Annotation group	Description	Genes in group
macrophage	actin, myosin, troponin	*acta1b, myl1, mylpf (2 of 2), mylz3, tnni2a.4, tpma*
	cathepsin L	*ctsl.1*
	colony stimulating factor 3	*csf3*
	granulins	*grn1, grn2*
	lectins	*hbl4, lgals1l1*
	leukocyte cell-derived chemotaxin 2 like	*lect2l*
	lysozyme g-like	*lygl1*
	mediator complex subunit	*med11(2 of 2)*
	MHC class II	*cd74*
	microfibrillar-associated proteins	*mfap4, zgc:173915, si:zfos-2330d3.3*
	nephrosin	*npsn*
	parvalbumins	*pvalb2, pvalb4*
	riboflavin kinase	*rfk*
	S100 calcium binding protein A11	*s100a11*
	transducin beta-like	*tbl2(1 of 2)*
	ubiquitin-like with PHD and ring finger domains 1	*uhrf1(1 of 2)*
translation	Finkel-Biskis-Reilly murine sarcoma virus (FBR-MuSV) ubiquitously expressed a	*faua*
	histones	*h3f3c, hist2h4b (7 of 7)*
	ribosomal proteins	*mrpl11, rpl13, rpl24, rpl28, rpl37, rps10, rps14, RPS17, rps19, rps21, rps26l, rps3*
	translation initiation factors	*eif2b2, eif3k*
	ubiquitin A-52 residue ribosomal protein fusion product 1 [Source:ZFIN;Acc:ZDB-GENE-051023-7]	*uba52*
	VAMP (vesicle-associated membrane protein)-associated protein A, like	*vapal*
oxidative phosphorylation	ATP synthases, H+ transporting, mitochondrial	*atp5d, atp5j*
	cytochrome c oxidase subunits	*cox5a (1 of 3), cox5ab, cox6a1*
	NADH dehydrogenase (ubiquinone)	*ndufa13, ndufa2, ndufa5, ndufa6, ndufb3, ndufb7, ndufb8, ndufb9, ndufs5, ndufs7, ndufv2, ndufv3*
	succinate dehydrogenase complex, subunit B, iron sulfur (Ip)	*sdhb*
proteolysis	elastases	*ela2, ela2l, ela3l*
	lon peptidase 1, mitochondrial	*lonp1*
	proteasome subunits	*psma1, psmb1, psmb2, psmb6, psmd3*
	trypsins	*ctrb1, ctrl, try*

ion transport/ion binding	ATP synthases, H+ transporting, mitochondrial	*atp5d, atp5j*
	betaine-homocysteine methyltransferase	*bhmt*
	hemoglobin zeta	*hbz*
	hepcidin antimicrobial peptide 1	*hamp1*
	myeloid cell leukemia sequence 1a	*mcl1a*
	potassium channel, subfamily K, member 10a	*kcnk10a*
	ribosomal protein L37	*rpl37*
	succinate dehydrogenase complex, subunit B, iron sulfur (Ip)	*sdhb*
	zinc finger-like gene 2a	*znfl2a*
chromatin organization	histones	*h3f3c, hist2h4b (7 of 7)*
	single-minded homolog 1	*sim1 (3 of 3)*
	SRY-box containing gene 19b	*sox19b*
lipid metabolism	apolipoproteins	*apoa1, apoa1 (2 of 2), apoc2*
	enolase 3	*eno3*
	fatty acid binding proteins	*fabp10a, fabp1b.1*
	phospholipase D family, member 3	*pld3*
lectins	galactoside-binding lectins	*lgals2b, lgals1l1*
	hexose-binding lectin 4	*hbl4*
	intelectin 3	*itln3*
	mannose-binding lectin 2-like	*lman2l (2 of 2)*
immunosuppression	FK506 (fkbp5) binding proteins	*fkbp11, fkbp3*
	vasoactive intestinal peptide	*vip (2 of 2)*

*Embryos were infected by intravenous injection of mCherry-labeled *M. marinum* Mma20 bacteria at 1 dpf, and at 4 dpi (5dpf) RNA-Seq libraries were prepared from mCherry-positive (+) and negative (-) cell fractions obtained by FACS-sorting. Read counts from two biological replicates of infected embryos were compared by DESeq analysis against the eGFP-negative cell fractions of two biological replicates of uninfected *mpeg1:egfp* larvae (5 dpf). Ensembl ID codes of 148 significantly enriched genes (log2 fold change > 2, adjusted P-value <0.1) in mCherry-positive Mma20-infected cells were analyzed using DAVID, which showed enrichment of five annotation clusters: translation, oxidative phosphorylation, proteolysis, ion transport/binding, and chromatin assembly. Furthermore, overlap with genes enriched in *mpeg1:egfp*-positive cells identified a macrophage gene group, and manual annotation identified three additional gene groups: lipid metabolism, lectins, and genes involved in immunosuppression. The full list of significantly enriched genes with fold change, P-value, and RPKM values of the biological replicates in given in Supplementary table 3.

Supplementary Table 5. Genes affected by *ptpn6* knockdown in *M. marinum*-infected cells and different leukocyte populations**.** Supplementary table can be found online at: https://www.dropbox.com/s/n4bjcjtfseraljp/Chapter3suppl.table5.xlsx

References

An, H., J. Hou, J. Zhou, W. Zhao, H. Xu, Y. Zheng, Y. Yu, S. Liu, and X. Cao. 'Phosphatase Shp-1 Promotes Tlr- and Rig-I-Activated Production of Type I Interferon by Inhibiting the Kinase Irak1', *Nature immunology* Vol. 9, No. 5, 542-50, 2008.

Anders, S., and W. Huber. 'Differential Expression Analysis for Sequence Count Data', *Genome biology* Vol. 11, No. 10, R106, 2010.

Beatty, W. L., E. R. Rhoades, D. K. Hsu, F. T. Liu, and D. G. Russell. 'Association of a Macrophage Galactoside-Binding Protein with Mycobacterium-Containing Phagosomes', *Cellular microbiology* Vol. 4, No. 3, 167-76, 2002.

Benard, E. L., A. M. van der Sar, F. Ellett, G. J. Lieschke, H. P. Spaink, and A. H. Meijer. 'Infection of Zebrafish Embryos with Intracellular Bacterial Pathogens', *Journal of visualized experiments : JoVE*, No. 61, 2012.

Blanchette, J., I. Abu-Dayyeh, K. Hassani, L. Whitcombe, and M. Olivier. 'Regulation of Macrophage Nitric Oxide Production by the Protein Tyrosine Phosphatase Src Homology 2 Domain Phosphotyrosine Phosphatase 1 (Shp-1)', *Immunology* Vol. 127, No. 1, 123-33, 2009.

Chaussabel, D., V. Pascual, and J. Banchereau. 'Assessing the Human Immune System through Blood Transcriptomics', *BMC biology* Vol. 8, 84, 2010.

Chen, E. S., Z. Song, M. H. Willett, S. Heine, R. C. Yung, M. C. Liu, S. D. Groshong, Y. Zhang, R. M. Tuder, and D. R. Moller. 'Serum Amyloid a Regulates Granulomatous Inflammation in Sarcoidosis through Toll-Like Receptor-2', *American journal of respiratory and critical care medicine* Vol. 181, No. 4, 360-73, 2010.

Clay, H., J. M. Davis, D. Beery, A. Huttenlocher, S. E. Lyons, and L. Ramakrishnan. 'Dichotomous Role of the Macrophage in Early Mycobacterium Marinum Infection of the Zebrafish', *Cell host & microbe* Vol. 2, No. 1, 29-39, 2007.

Cloonan, N., A. R. Forrest, G. Kolle, B. B. Gardiner, G. J. Faulkner, M. K. Brown, D. F. Taylor, A. L. Steptoe, S. Wani, G. Bethel, A. J. Robertson, A. C. Perkins, S. J. Bruce, C. C. Lee, S. S. Ranade, H. E. Peckham, J. M. Manning, K. J. McKernan, and S. M. Grimmond. 'Stem Cell Transcriptome Profiling Via Massive-Scale Mrna Sequencing', *Nature methods* Vol. 5, No. 7, 613-9, 2008.

Croker, B. A., B. R. Lawson, S. Rutschmann, M. Berger, C. Eidenschenk, A. L. Blasius, E. M. Moresco, S. Sovath, L. Cengia, L. D. Shultz, A. N. Theofilopoulos, S. Pettersson, and B. A. Beutler. 'Inflammation and Autoimmunity Caused by a Shp1 Mutation Depend on Il-1, Myd88, and a Microbial Trigger', *Proceedings of the National Academy of Sciences of the United States of America* Vol. 105, No. 39, 15028-33, 2008.

Cui, C., E. L. Benard, Z. Kanwal, O. W. Stockhammer, M. van der Vaart, A. Zakrzewska, H. P. Spaink, and A. H. Meijer. 'Infectious Disease Modeling and Innate Immune Function in Zebrafish Embryos', *Methods in cell biology* Vol. 105, 273-308, 2011.

Davis, J. M., H. Clay, J. L. Lewis, N. Ghori, P. Herbomel, and L. Ramakrishnan. 'Real-Time Visualization of Mycobacterium-Macrophage Interactions Leading to Initiation of Granuloma Formation in Zebrafish Embryos', *Immunity* Vol. 17, No. 6, 693-702, 2002.

Davis, J. M., and L. Ramakrishnan. 'The Role of the Granuloma in Expansion and Dissemination of Early Tuberculous Infection', *Cell* Vol. 136, No. 1, 37-49, 2009.

Denholm, J. T., E. S. McBryde, and D. P. Eisen. 'Mannose-Binding Lectin and Susceptibility to Tuberculosis: A Meta-Analysis', *Clinical and experimental immunology* Vol. 162, No. 1, 84-90, 2010.

Ellett, F., and G. J. Lieschke. 'Zebrafish as a Model for Vertebrate Hematopoiesis', *Current opinion in pharmacology* Vol. 10, No. 5, 563-70, 2010.

Ellett, F., L. Pase, J. W. Hayman, A. Andrianopoulos, and G. J. Lieschke. 'Mpeg1 Promoter Transgenes Direct Macrophage-Lineage Expression in Zebrafish', *Blood* Vol. 117, No. 4, e49-56, 2011.

Fullwood, M. J., C. L. Wei, E. T. Liu, and Y. Ruan. 'Next-Generation DNA Sequencing of Paired-End Tags (Pet) for Transcriptome and Genome Analyses', *Genome research* Vol. 19, No. 4, 521-32, 2009.

Gao, X., and P. R. Hardwidge. 'Ribosomal Protein S3: A Multifunctional Target of Attaching/Effacing Bacterial Pathogens', *Frontiers in microbiology* Vol. 2, 137, 2011.

Hall, C., M. V. Flores, A. Chien, A. Davidson, K. Crosier, and P. Crosier. 'Transgenic Zebrafish Reporter Lines Reveal Conserved Toll-Like Receptor Signaling Potential in Embryonic Myeloid Leukocytes and Adult Immune Cell Lineages', *Journal of leukocyte biology* Vol. 85, No. 5, 751-65, 2009.

Hardcastle, T. J., and K. A. Kelly. 'Bayseq: Empirical Bayesian Methods for Identifying Differential Expression in Sequence Count Data', *BMC bioinformatics* Vol. 11, 422, 2010.

Hegedus, Z., A. Zakrzewska, V. C. Agoston, A. Ordas, P. Racz, M. Mink, H. P. Spaink, and A. H. Meijer. 'Deep Sequencing of the Zebrafish Transcriptome Response to Mycobacterium Infection', *Molecular immunology* Vol. 46, No. 15, 2918-30, 2009.

Henshall, T. L., K. L. Jones, R. Wilkinson, and D. E. Jackson. 'Src Homology 2 Domain-Containing Protein-Tyrosine Phosphatases, Shp-1 and Shp-2, Are Required for Platelet Endothelial Cell Adhesion Molecule-1/Cd31-Mediated Inhibitory Signaling', *Journal of immunology* Vol. 166, No. 5, 3098-106, 2001.

Herbomel, P., B. Thisse, and C. Thisse. 'Ontogeny and Behaviour of Early Macrophages in the Zebrafish Embryo', *Development* Vol. 126, No. 17, 3735-45, 1999.

Huang da, W., B. T. Sherman, and R. A. Lempicki. 'Systematic and Integrative Analysis of Large Gene Lists Using David Bioinformatics Resources', *Nature protocols* Vol. 4, No. 1, 44-57, 2009.

Janeway, C. A., Jr., and R. Medzhitov. 'Innate Immune Recognition', *Annual review of immunology* Vol. 20, 197-216, 2002.

Kim, M. J., H. C. Wainwright, M. Locketz, L. G. Bekker, G. B. Walther, C. Dittrich, A. Visser, W. Wang, F. F. Hsu, U. Wiehart, L. Tsenova, G. Kaplan, and D. G. Russell. 'Caseation of Human Tuberculosis Granulomas Correlates with Elevated Host Lipid Metabolism', *EMBO molecular medicine* Vol. 2, No. 7, 258-74, 2010.

Kissa, K., E. Murayama, A. Zapata, A. Cortes, E. Perret, C. Machu, and P. Herbomel. 'Live Imaging of Emerging Hematopoietic Stem Cells and Early Thymus Colonization', *Blood* Vol. 111, No. 3, 1147-56, 2008.

Kumagai, C., B. Kalman, F. A. Middleton, T. Vyshkina, and P. T. Massa. 'Increased Promoter Methylation of the Immune Regulatory Gene Shp-1 in Leukocytes of Multiple Sclerosis Subjects', *Journal of neuroimmunology* Vol. 246, No. 1-2, 51-7, 2012.

Lam, S. H., H. L. Chua, Z. Gong, T. J. Lam, and Y. M. Sin. 'Development and Maturation of the Immune System in Zebrafish, Danio Rerio: A Gene Expression Profiling, in Situ Hybridization and Immunological Study', *Developmental and comparative immunology* Vol. 28, No. 1, 9-28, 2004.

Langenau, D. M., A. A. Ferrando, D. Traver, J. L. Kutok, J. P. Hezel, J. P. Kanki, L. I. Zon, A. T. Look, and N. S. Trede. 'In Vivo Tracking of T Cell Development, Ablation, and Engraftment in Transgenic Zebrafish', *Proceedings of the National Academy of Sciences of the United States of America* Vol. 101, No. 19, 7369-74, 2004.

Lawson, N. D., and S. A. Wolfe. 'Forward and Reverse Genetic Approaches for the Analysis of Vertebrate Development in the Zebrafish', *Developmental cell* Vol. 21, No. 1, 48-64, 2011.

Le Guyader, D., M. J. Redd, E. Colucci-Guyon, E. Murayama, K. Kissa, V. Briolat, E. Mordelet, A. Zapata, H. Shinomiya, and P. Herbomel. 'Origins and Unconventional Behavior of Neutrophils in Developing Zebrafish', *Blood* Vol. 111, No. 1, 132-41, 2008.

Lee, H. Y., M. K. Kim, K. S. Park, Y. H. Bae, J. Yun, J. I. Park, J. Y. Kwak, and Y. S. Bae. 'Serum Amyloid a Stimulates Matrix-Metalloproteinase-9 Upregulation Via Formyl Peptide Receptor Like-1-Mediated Signaling in Human Monocytic Cells', *Biochemical and biophysical research communications* Vol. 330, No. 3, 989-98, 2005.

Lemos, M. P., K. Y. Rhee, and J. D. McKinney. 'Expression of the Leptin Receptor Outside of Bone Marrow-Derived Cells Regulates Tuberculosis Control and Lung Macrophage Mhc Expression', *Journal of immunology* Vol. 187, No. 7, 3776-84, 2011.

Ma, J., T. Chen, J. Mandelin, A. Ceponis, N. E. Miller, M. Hukkanen, G. F. Ma, and Y. T. Konttinen. 'Regulation of Macrophage Activation', *Cellular and molecular life sciences : CMLS* Vol. 60, No. 11, 2334-46, 2003.

Malle, E., S. Sodin-Semrl, and A. Kovacevic. 'Serum Amyloid A: An Acute-Phase Protein Involved in Tumour Pathogenesis', *Cellular and molecular life sciences : CMLS* Vol. 66, No. 1, 9-26, 2009.

Malone, J. H., and B. Oliver. 'Microarrays, Deep Sequencing and the True Measure of the Transcriptome', *BMC biology* Vol. 9, 34, 2011.

Marioni, J. C., C. E. Mason, S. M. Mane, M. Stephens, and Y. Gilad. 'Rna-Seq: An Assessment of Technical Reproducibility and Comparison with Gene Expression Arrays', *Genome research* Vol. 18, No. 9, 1509-17, 2008.

Martin, J. A., and Z. Wang. 'Next-Generation Transcriptome Assembly', *Nature reviews. Genetics* Vol. 12, No. 10, 671-82, 2011.

Meeker, N. D., and N. S. Trede. 'Immunology and Zebrafish: Spawning New Models of Human Disease', *Developmental and comparative immunology* Vol. 32, No. 7, 745-57, 2008.

Meijer, A. H., and H. P. Spaink. 'Host-Pathogen Interactions Made Transparent with the Zebrafish Model', *Current drug targets* Vol. 12, No. 7, 1000-17, 2011.

Mortazavi, A., B. A. Williams, K. McCue, L. Schaeffer, and B. Wold. 'Mapping and Quantifying Mammalian Transcriptomes by Rna-Seq', *Nature methods* Vol. 5, No. 7, 621-8, 2008.

Nagalakshmi, U., Z. Wang, K. Waern, C. Shou, D. Raha, M. Gerstein, and M. Snyder. 'The Transcriptional Landscape of the Yeast Genome Defined by Rna Sequencing', *Science* Vol. 320, No. 5881, 1344-9, 2008.

Oehlers, S. H., M. V. Flores, C. J. Hall, S. Swift, K. E. Crosier, and P. S. Crosier. 'The Inflammatory Bowel Disease (Ibd) Susceptibility Genes Nod1 and Nod2 Have Conserved Anti-Bacterial Roles in Zebrafish', *Disease models & mechanisms* Vol. 4, No. 6, 832-41, 2011.

Oh, S. Y., T. Zheng, Y. K. Kim, L. Cohn, R. J. Homer, A. N. McKenzie, and Z. Zhu. 'A Critical Role of Shp-1 in Regulation of Type 2 Inflammation in the Lung', *American journal of respiratory cell and molecular biology* Vol. 40, No. 5, 568-74, 2009.

Ordas, A., Z. Hegedus, C. V. Henkel, O. W. Stockhammer, D. Butler, H. J. Jansen, P. Racz, M. Mink, H. P. Spaink, and A. H. Meijer. 'Deep Sequencing of the Innate Immune Transcriptomic Response of Zebrafish Embryos to Salmonella Infection', *Fish & shellfish immunology* Vol. 31, No. 5, 716-24, 2011.

Ramakrishnan, L. 'Revisiting the Role of the Granuloma in Tuberculosis', *Nature reviews. Immunology* Vol. 12, No. 5, 352-66, 2012.

Ray, A., B. S. Bal, and B. K. Ray. 'Transcriptional Induction of Matrix Metalloproteinase-9 in the Chondrocyte and Synoviocyte Cells Is Regulated Via a Novel Mechanism: Evidence for Functional Cooperation between Serum Amyloid a-Activating Factor-1 and Ap-1', *Journal of immunology* Vol. 175, No. 6, 4039-48, 2005.

Renshaw, S. A., C. A. Loynes, S. Elworthy, P. W. Ingham, and M. K. Whyte. 'Modeling Inflammation in the Zebrafish: How a Fish Can Help Us Understand Lung Disease', *Experimental lung research* Vol. 33, No. 10, 549-54, 2007.

Renshaw, S. A., C. A. Loynes, D. M. Trushell, S. Elworthy, P. W. Ingham, and M. K. Whyte. 'A Transgenic Zebrafish Model of Neutrophilic Inflammation', *Blood* Vol. 108, No. 13, 3976-8, 2006.

Renshaw, S. A., and N. S. Trede. 'A Model 450 Million Years in the Making: Zebrafish and Vertebrate Immunity', *Disease models & mechanisms* Vol. 5, No. 1, 38-47, 2012.

Robinson, M. D., D. J. McCarthy, and G. K. Smyth. 'Edger: A Bioconductor Package for Differential Expression Analysis of Digital Gene Expression Data', *Bioinformatics* Vol. 26, No. 1, 139-40, 2010.

Russell, D. G. 'Mycobacterium Tuberculosis and the Intimate Discourse of a Chronic Infection', *Immunological reviews* Vol. 240, No. 1, 252-68, 2011.

Singla, N., D. Gupta, A. Joshi, N. Batra, J. Singh, and N. Birbian. 'Association of Mannose-Binding Lectin Gene Polymorphism with Tuberculosis Susceptibility and Sputum Conversion Time', *International journal of immunogenetics* Vol. 39, No. 1, 10-4, 2012.

Souza-Moreira, L., J. Campos-Salinas, M. Caro, and E. Gonzalez-Rey. 'Neuropeptides as Pleiotropic Modulators of the Immune Response', *Neuroendocrinology* Vol. 94, No. 2, 89-100, 2011.

Sow, F. B., W. C. Florence, A. R. Satoskar, L. S. Schlesinger, B. S. Zwilling, and W. P. Lafuse. 'Expression and Localization of Hepcidin in Macrophages: A Role in Host Defense against Tuberculosis', *Journal of leukocyte biology* Vol. 82, No. 4, 934-45, 2007.

Sow, F. B., S. Nandakumar, V. Velu, K. L. Kellar, L. S. Schlesinger, R. R. Amara, W. P. Lafuse, T. M. Shinnick, and S. B. Sable. 'Mycobacterium Tuberculosis Components Stimulate Production of the Antimicrobial Peptide Hepcidin', *Tuberculosis* Vol. 91, No. 4, 314-21, 2011.

Stockhammer, O. W., H. Rauwerda, F. R. Wittink, T. M. Breit, A. H. Meijer, and H. P. Spaink. 'Transcriptome Analysis of Traf6 Function in the Innate Immune Response of Zebrafish Embryos', *Molecular immunology* Vol. 48, No. 1-3, 179-90, 2010.

Stockhammer, O. W., A. Zakrzewska, Z. Hegedus, H. P. Spaink, and A. H. Meijer. 'Transcriptome Profiling and Functional Analyses of the Zebrafish Embryonic Innate Immune Response to Salmonella Infection', *Journal of immunology* Vol. 182, No. 9, 5641-53, 2009.

Sultan, M., M. H. Schulz, H. Richard, A. Magen, A. Klingenhoff, M. Scherf, M. Seifert, T. Borodina, A. Soldatov, D. Parkhomchuk, D. Schmidt, S. O'Keeffe, S. Haas, M. Vingron, H. Lehrach, and M. L. Yaspo. 'A Global View of Gene Activity and Alternative Splicing by Deep Sequencing of the Human Transcriptome', *Science* Vol. 321, No. 5891, 956-60, 2008.

Ten Freyhaus, H., E. S. Calay, A. Yalcin, S. N. Vallerie, L. Yang, Z. Z. Calay, F. Saatcioglu, and G. S. Hotamisligil. 'Stamp2 Controls Macrophage Inflammation through Nicotinamide Adenine Dinucleotide Phosphate Homeostasis and Protects against Atherosclerosis', *Cell metabolism* Vol. 16, No. 1, 81-9, 2012.

Tobin, D. M., F. J. Roca, S. F. Oh, R. McFarland, T. W. Vickery, J. P. Ray, D. C. Ko, Y. Zou, N. D. Bang, T. T. Chau, J. C. Vary, T. R. Hawn, S. J. Dunstan, J. J. Farrar, G. E. Thwaites, M. C. King, C. N. Serhan, and L. Ramakrishnan. 'Host Genotype-Specific Therapies Can Optimize the Inflammatory Response to Mycobacterial Infections', *Cell* Vol. 148, No. 3, 434-46, 2012.

Trapnell, C., B. A. Williams, G. Pertea, A. Mortazavi, G. Kwan, M. J. van Baren, S. L. Salzberg, B. J. Wold, and L. Pachter. 'Transcript Assembly and Quantification by Rna-Seq Reveals Unannotated Transcripts and Isoform Switching During Cell Differentiation', *Nature biotechnology* Vol. 28, No. 5, 511-5, 2010.

van der Sar, A. M., A. M. Abdallah, M. Sparrius, E. Reinders, C. M. Vandenbroucke-Grauls, and W. Bitter. 'Mycobacterium Marinum Strains Can Be Divided into Two Distinct Types Based on Genetic Diversity and Virulence', *Infection and immunity* Vol. 72, No. 11, 6306-12, 2004.

van der Sar, A. M., H. P. Spaink, A. Zakrzewska, W. Bitter, and A. H. Meijer. 'Specificity of the Zebrafish Host Transcriptome Response to Acute and Chronic Mycobacterial Infection and the Role of Innate and Adaptive Immune Components', *Molecular immunology* Vol. 46, No. 11-12, 2317-32, 2009.

van Soest, J. J., O. W. Stockhammer, A. Ordas, G. V. Bloemberg, H. P. Spaink, and A. H. Meijer. 'Comparison of Static Immersion and Intravenous Injection Systems for Exposure of Zebrafish Embryos to the Natural Pathogen Edwardsiella Tarda', *BMC immunology* Vol. 12, 58, 2011.

Volkman, H. E., T. C. Pozos, J. Zheng, J. M. Davis, J. F. Rawls, and L. Ramakrishnan. 'Tuberculous Granuloma Induction Via Interaction of a Bacterial Secreted Protein with Host Epithelium', *Science* Vol. 327, No. 5964, 466-9, 2010.

Wang, L., Z. Feng, X. Wang, and X. Zhang. 'Degseq: An R Package for Identifying Differentially Expressed Genes from Rna-Seq Data', *Bioinformatics* Vol. 26, No. 1, 136-8, 2010.

Wang, Z., M. Gerstein, and M. Snyder. 'Rna-Seq: A Revolutionary Tool for Transcriptomics', *Nature reviews. Genetics* Vol. 10, No. 1, 57-63, 2009.

Wellen, K. E., R. Fucho, M. F. Gregor, M. Furuhashi, C. Morgan, T. Lindstad, E. Vaillancourt, C. Z. Gorgun, F. Saatcioglu, and G. S. Hotamisligil. 'Coordinated Regulation of Nutrient and Inflammatory Responses by Stamp2 Is Essential for Metabolic Homeostasis', *Cell* Vol. 129, No. 3, 537-48, 2007.

Wieland, C. W., S. Florquin, E. D. Chan, J. C. Leemans, S. Weijer, A. Verbon, G. Fantuzzi, and T. van der Poll. 'Pulmonary Mycobacterium Tuberculosis Infection in Leptin-Deficient Ob/Ob Mice', *International immunology* Vol. 17, No. 11, 1399-408, 2005.

Zakrzewska, A., C. Cui, O. W. Stockhammer, E. L. Benard, H. P. Spaink, and A. H. Meijer. 'Macrophage-Specific Gene Functions in Spi1-Directed Innate Immunity', *Blood* Vol. 116, No. 3, e1-11, 2010.